

Microwave-Accelerated Plasmonics: Application to Ultra-Fast and Ultra-Sensitive Clinical Assays

Kadir Aslan^a, Michael J.R. Previte^a, Yongxia Zhang^a and Chris D. Geddes^{a,b,*}

^a Institute of Fluorescence, Laboratory for Advanced Medical Plasmonics, Medical Biotechnology Center, University of Maryland Biotechnology Institute, 725 West Lombard St, Baltimore, MD, 21201, USA.

^b Center for Fluorescence Spectroscopy, Department of Biochemistry and Molecular Biology, Medical Biotechnology Center, University of Maryland School of Medicine, 725 West Lombard St, Baltimore, MD, 21201, USA

ABSTRACT

In recent years our laboratory has described the favorable effects of fluorophores in close proximity to metallic nanostructures (1-6). These include, increased system quantum yields (increased detectability) and much improved fluorophore photostabilities. These effects have led to many applications of metal-enhanced fluorescence (MEF) including, improved DNA detection (7, 8), enhanced ratiometric sensing (5), metal-enhanced phosphorescence (9) and chemiluminescence signatures (10), as well as to the development of nano-rod (6), triangular nano-plate (4) and modified plastic surfaces (1, 3) for their multifarious applications. In all of our applications of MEF to date, we have been able to significantly optically amplify luminescence based signatures, but have been unable to modify the rates of the respective biochemical reactions being either studied or utilized, as these are dependent on the usual solution parameters of temperature, viscosity and their bioaffinity etc.

However, our laboratory has recently shown that low power microwaves, when applied to the metallic nanostructures which are suitable for MEF, are preferentially heated, rapidly accelerating local biochemical reactions (11). Subsequently, ultra-fast and ultra-sensitive assays can be realized. We have recently termed the amalgamation of both MEF with microwave heating as “Microwave-Accelerated Metal-Enhanced Fluorescence (MAMEF)”. In this conference proceeding, we summarize our MAMEF work on ultra-fast and sensitive myoglobin detection for rapid cardiac risk assessment and DNA detection for bioterrorism applications. In addition we present two new platform technologies, namely, Microwave-Accelerated Surface Plasmon-Coupled Directional Luminescence (MA-SPCL) for ultra fast assays using clinical samples and a Microwave-Accelerated Aggregation Assay (MA-AA) technology, for ultra fast solution-based nanoparticle aggregation assays.

Keywords: Metal-Enhanced Fluorescence, Microwave-Accelerated Metal-Enhanced Fluorescence, Silver Colloids, Fast Assays, DNA detection, Anthrax, Cardiac Risk Assessment, Myoglobin, Plasmon Controlled Fluorescence, Microwave-Accelerated Plasmonics, Surface Enhanced Fluorescence, Plasmon Enhanced Fluorescence.

1. INTRODUCTION

Fluorescence detection is the basis of most assays used in drug discovery, high throughput screening (HTS) and medical diagnostics today. In all of these assays, assay rapidity and sensitivity is a primary concern, the sensitivity determined by both the quantum yield of the fluorophores and efficiency of the detection system, while rapidity is determined by the physical and biophysical parameters of temperature, concentration, assay bioaffinity etc.

Metal-Enhanced Fluorescence, a technology that has been extensively studied over the last 5 years (1-6), allows scientists to address issues of assay sensitivity. In MEF, fluorescence emission from a fluorophore placed near to silver nanostructures will be significantly increased; this benefit of MEF is demonstrated in Figure 1-Left: a greater fluorescence emission is observed from fluorophores adsorbed on to silver nanoparticles as compared to glass alone. Specifically, the excited fluorophores partially transfer energy to the silver nanoparticles, where the energy in essence is amplified, as the emission from the fluorophore-silver “system” becomes more efficient than the emission from the

* geddes@umbi.umd.edu; phone 1 410 706-3149; fax 1 410 706-4600

fluorophores alone (Figure 1-Right) (12). MEF also results in a reduced lifetime of the fluorophore, a consequence being that the fluorophores are more photostable. It is this unique combination of an increased emission intensity, coupled with a reduced lifetime that has recently lead to the use of MEF in many biotechnological applications; such as in the increased detectability and photostability of fluorophores (2), improved DNA detection (8), and the application of metallic surfaces to amplified wavelength-ratiometric sensing (5) to name a few.

The use of MEF addresses the issue of immunoassay sensitivity. However, most biological recognition events, such as an antigen-antibody interaction or DNA hybridization are often kinetically slow, requiring long incubation times. As a result very few immunoassays can be completed in less than 10 minutes (13). In this regard, a new platform technology, Microwave-Accelerated Metal-Enhanced Fluorescence (MA-MEF) which couples the benefits of MEF with the use of low power microwaves, to accelerate bioaffinity reactions was recently introduced by us for bioassays (11), DNA hybridization (14) and immunoassays (15). In the MA-MEF technology, the MEF phenomenon increases the sensitivity



Fig. 1. (Left) Photographs: Silver Island Films (SiFs) deposited glass substrate and real color emission of TAMRA on glass and SiFs taken through a 532 nm notch filter. (Right) Interpretation of metal-enhanced fluorescence (MEF) phenomenon whereby fluorescence emission from the fluorophores is partially plasmon coupled and the system (fluorophore and SiFs) radiates. TAMRA-tetramethylrhodamine.

of the assays while the use of low power microwave heating kinetically accelerates assays to completion within seconds. In this conference proceeding, we therefore summarize our findings of a new platform technology that promises to fundamentally address these two physical constraints of sensitivity and rapidity. By combining the use of MEF, a near-field effect that can significantly enhance fluorescence signatures, with low power microwave heating, we can significantly increase the sensitivity of surface assays as well as > 95 % kinetically complete the assay within a few seconds. In addition, the metallic nanostructures used to facilitate MEF, appear to localize heating as compared to the surface assay fluid, advantageously localizing the MEF and heating around the nanostructures.

2. METHODOLOGY

Since this proceeding summarizes the results from seven of our previously published (or in press) works and due to the page limitations here, we refer the reader to the cited papers for details of the experimental procedure for each result. Here, we present the general experimental procedures for all works.

2.1 Formation of silver island films (SiFs) on glass substrates

In a typical SiFs preparation a solution of silver nitrate (0.5 g in 60 ml of deionized water) in a clean 100-ml glass beaker, equipped with a Teflon-coated stir bar, is prepared and placed on a Corning stirring/hot plate. While stirring at the quickest speed, 8 drops ($\approx 200 \mu\text{L}$) of freshly prepared 5% (w/v) sodium hydroxide solution are added. This results in the formation of dark brown precipitates of silver particles. Approximately 2 ml of ammonium hydroxide is then added, drop by drop, to re-dissolve the precipitates. The clear solution is cooled to 5°C by placing the beaker in an ice bath, followed by soaking the 3-aminopropyltrithoxysilane (APS)-coated glass slides in the solution. While keeping the slides at 5°C , a fresh solution of *D*-glucose (0.72 g in 15 ml of water) is added. Subsequently, the temperature of the mixture is then warmed to 30°C . As the color of the mixture turns from yellow-green to yellow-brown, and the color of the slides become green, the slides are removed from the mixture, washed with water, and sonicated for 1 minute at room temperature. SiFs-deposited slides were then rinsed with deionized water several times and dried under a stream of nitrogen gas.

2.2 Synthesis of Silver Colloids and the Coating of High Throughput Screening (HTS) Wells with Silver Colloid Films

The synthesis of silver colloids was performed using the following procedure: 2 ml of 1.16 mM trisodium citrate solution was added drop wise to a heated (90°C) 98 ml aqueous solution of 0.65 mM of silver nitrate while stirring. The mixture was kept heated for 10 minutes, and then it was cooled to room temperature.

The coating of the HTS plates was achieved by incubating 0.5 ml of silver colloid solution inside the HTS wells (48 wells) overnight. The HTS wells were coated with silver colloids due to the binding of silver to the amine groups of the surface poly-lysine (Malicka et al., 2003), as demonstrated previously by our laboratories. The other half of the wells (48 wells) in the same HTS plates were left intentionally blank for the control experiments. The silver colloid deposited HTS wells were rinsed with deionized water several times prior to the fluorescence experiments.

2.3 Preparation of Biotinylated BSA-coated 20 nm Gold Colloids

The surface modification of 20 nm gold colloids was performed using an adapted version of the procedure found in the literature (16). In this regard, 5 mL of the gold colloids solution was mixed with 0.05 mL aqueous solution of biotinylated BSA (1.44 mg / mL), and this mixture was incubated at room temperature for 2 hours. The gold colloids / biotinylated BSA mixture was then centrifuged in an Eppendorf centrifuge tube equipped with a 100,000 MW cut-off filter for 10 minutes, using an Eppendorf microcentrifuge at 8,000g, to separate the biotinylated BSA-coated gold colloids from the excess biotinylated BSA. The supernatant was carefully removed, and the pellet containing the biotinylated gold colloids was resuspended in 10 mM sodium phosphate buffer (pH 7). This was subsequently used in the aggregation assays.

2.4 Absorption and Fluorescence Measurements

All absorption measurements were performed using a HP 8453 UV-Vis spectrophotometer. Fluorescence measurements on HTS plates were performed by placing the HTS plates on a Total Internal Reflection (TIR) stage equipped with a fiber-optic mount on a 15-cm-long arm (not shown here). The output of the fiber was connected to an Ocean Optics HD2000 spectrofluorometer to measure the fluorescence emission spectra. The excitation was from the second harmonic (473 nm or 532 nm) of the diode-pumped Nd:YVO4 laser (output power \approx 30 mW) at an angle of 45 degrees. This configuration allowed easy changes of the incident angle and the evanescent excitation spot position. The emission was observed through a 488 or 532 nm razor-edge filter (Semrock).

3. RESULTS AND DISCUSSION

3.1 Effects of Microwave Heating on Silver Nanoparticles

Figure 2 shows the plasmon absorption spectra of Silver Island Films (SiFs), both before and after low power microwave heating for 30 seconds. The cavity power was approximately 140 watts, which is the same as utilized in the assays discussed later, and is of a similar power used for immunostaining. As can be seen from Figure 2, the microwaves and heating had no effect on the surface plasmon absorption of the SiFs, indicating no structural or surface silver shape changes, where the surface plasmon absorption is well-known to be characteristic of the shape of the nanoparticles (17), which is due to the mean free path oscillation of surface charges. Furthermore no “sparking” was evident from the silvered surfaces, a known consequence of surface charge build-up and dissipation (18), for large non-wavelength sized particles or continuous surfaces .

We additionally measured the structural morphology of the silvered surfaces using Atomic Force Microscopy, Figure 2. While it is somewhat difficult to probe that exact same area after microwave heating, very little, if no change in surface morphology was observed between the locations. We additionally exposed the silvered surfaces, both wet and dry, to several hundreds watts of microwave cavity power over many minutes (data not shown). In all of these investigations no evidence for surface structural changes was found by microwave heating, clearly demonstrating the compatibility of the nanostructured surfaces to microwave exposure and therefore heating. In this

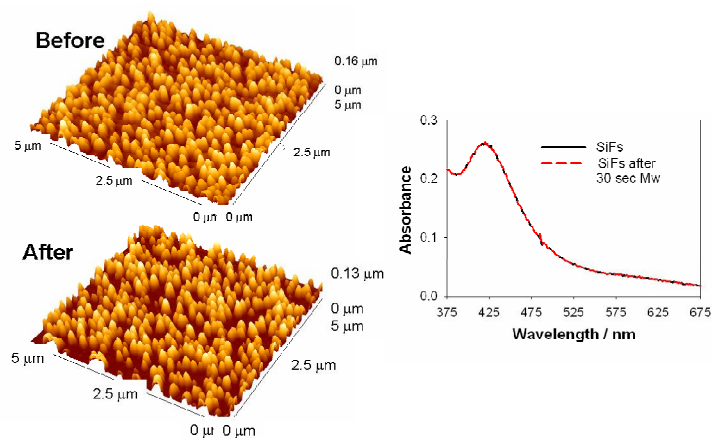


Fig. 2 - AFM images both before and after microwave heating (Left-Top and Left-Middle, respectively) and the corresponding plasmon absorption spectrum (Right). Adapted from reference 11.

regard, our laboratories have recently reported the Thermal Annealing of SiFs and its subsequent effect on the MEF effect (12), where changes in the surface morphology only occur at very high temperatures, i.e. > 200 °C.

3.2 Proof-of-Principle of Microwave-Accelerated Metal Enhanced Fluorescence Platform Technology

To demonstrate proof of principle that our MAMEF approach can be applied to high-throughput formats (as well as SiFs), we have used commercially available 96- well plates, with silver deposited on the bottom of the plates, Figure 3. Silver colloids can be readily deposited on the bottom of the clear plastic plates, the number density determined by the incubation conditions, the colloid size determined by the experimental conditions of preparation, all monitored by measuring the surface plasmon absorption (data not shown, see reference (19)).

The model protein system chosen was the Biotin-Avidin system, where the simple kinetics and bioaffinity of both for each other is well-known (20). Earlier studies by our laboratories had shown that biotinylated-BSA readily forms an equal monolayer on both silver and plastic substrates (1, 12). Subsequently, biotinylated BSA was coated on all 96-well plates, half of which had been silvered, the other half poly-lysine coated bare plastic, acting as control samples by which to compare the benefits of using the metal-enhanced fluorescence (MEF) phenomenon (2). The enhancement ratio I_{SiFs}/I_{HTS} (the benefit of using MEF) is the fluorescence intensity observed on the silver colloids divided by the intensity on the non-silvered substrate. In addition, this model protein system, Figure 3-Top, positions the fluorophore (which is fluorescein labeled avidin), > 4 nm from the surfaces.

Figure 3-Bottom shows the fluorescein emission intensity from both silvered and non-silvered HTS wells after room temperature incubation of the assay. The assay was incubated for 30 mins. The emission, which was collected through a 488 nm razor edge filter, shows an approximate 5 fold greater intensity from the silver as compared to the non-silvered wells. These values were the mean of 4 wells each. This increase is not due to reflected photons from the silvered surface, i.e. scattering, but is in fact a consequence of a new near-field fluorescence phenomenon reported by the authors (21), whereby fluorophores in close proximity (< 10 nm) to a silver nanostructures can be made highly fluorescent, i.e., MEF.

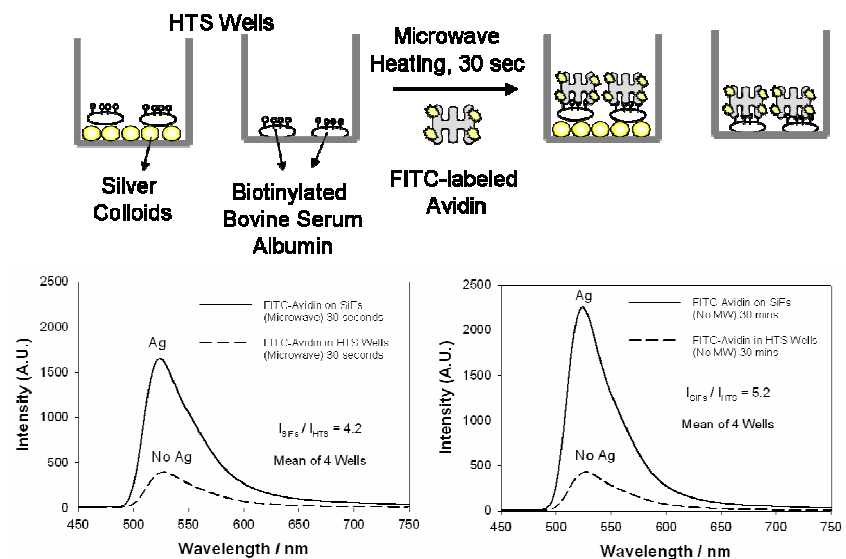


Fig. 3. Top-Model protein-fluorophore system used to demonstrate Microwave-Accelerated Metal-Enhanced Fluorescence (MAMEF). Both silvered and *unsilvered* HTS wells are equally coated with biotinylated-BSA. Fluorescein labeled avidin (FITC-Avidin) rapidly binds to the biotinylated-BSA within seconds after microwave heating while the same reaction takes 30 minutes at room temperature without microwave heating. Fluorescence emission intensity of fluorescein from both silvered and non-silvered HTS wells after 30 seconds microwave heating (Bottom-Left) after 30 mins room temperature incubation (Bottom Right). Adapted from reference 19.

3.3 Effects of Microwave Heating on Protein Confirmation

Since there is both considerable work and debate concerning DNA or protein damage upon exposure of organisms to microwaves (22), we investigated whether exposure to microwaves indeed caused protein denaturation in our model assay system. Protein conformational changes on the surface of a metal-enhanced fluorescence assay could potentially complicate assay kinetics and sensitivity, given that MEF is a through space and distance dependent phenomenon (2). Subsequently, we employed Fluorescence Resonance Energy Transfer (FRET) to investigate any protein conformational changes, a technique which is widely used (23). To investigate this, Fluorescein (Donor) and Alexa 532 (Acceptor) labeled avidin were incubated on surfaces both separately, together and both before and after microwave heating, Figure 4. In Figure 4-Left, we can see that the emission spectral properties of fluorescein labeled avidin incubated on to a

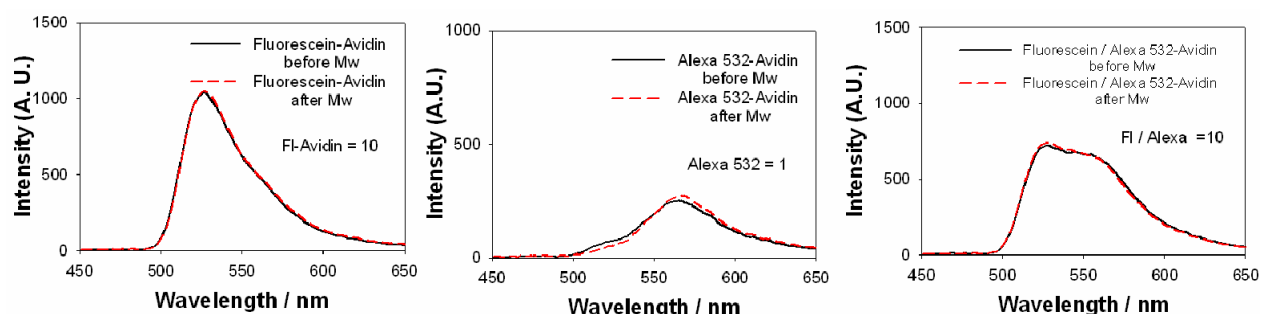


Fig. 4. Fluorescence resonance energy transfer experiments to confirm that the proteins are not denatured by low power microwaves. (Left) – Fluorescein (Donor) labeled avidin before and after low power microwave heating, (Middle) – Alexa 532 (Acceptor) labeled avidin before and after low power microwave heating, (Right) – Donor-acceptor labeled avidin (ratio D/A = 1) before and after low power microwave heating. The extent of energy transfer does not change after heating, suggesting that the proteins are not denatured. Adapted from reference 11.

biotinylated-BSA surface both before and after microwave heating remain unchanged. Similarly the acceptor (Alexa 532) incubated alone on the biotinylated surface shows no change in its emission spectral properties, Figure 4-Middle. When both the donor and acceptor were incubated together (30 mins) on the surface with a D/A ratio of 10:1, then we can clearly see both the Fluorescein emission and the Alexa emission, after sole excitation of the donor, Figure 4-Right. Interestingly, the emission spectra are identical both *before and after microwave heating*, suggesting that the surface protein assay has not undergone any conformational changes, where such changes would alter the FRET pair emission spectra. This strongly suggests that our approach using low power microwave heating does not modify surface assay morphology.

3.4 MAMEF-based Myoglobin Detection on Silvered Surfaces: Potential Application to Myocardial Infarction Diagnosis (Protein Detection)

To demonstrate the utility and clinical relevance of our new MAMEF approach for myoglobin detection we constructed a 2-stage assay as shown in Figure 5-Top. Firstly, the assay surface is prepared on both glass and silvered glass substrates, the glass substrate used as a control sample by which to compare the usefulness of the silver nanostructures. 100 ng/ml of myoglobin was subsequently washed over the assay surface followed by incubation of the anti-myoglobin antibody labeled Alexa 647 fluorophore. Figure 5-Bottom shows the emission spectra of the labeled Alexa-647 from both the glass and silvered glass regions of the slide, after the anti-myoglobin had been incubated at room temperature for 30 minutes. A careful investigation of the system has shown that the assay was $\approx 95\%$ kinetically complete after 30 minutes incubation at 20 C. From Figure 5-Bottom we can see a ≈ 7.5 fold increase in Alexa 647 emission on the silvered surface, as compared to the glass control, where the spectra shown are the mean of 5 separate surface measurements.

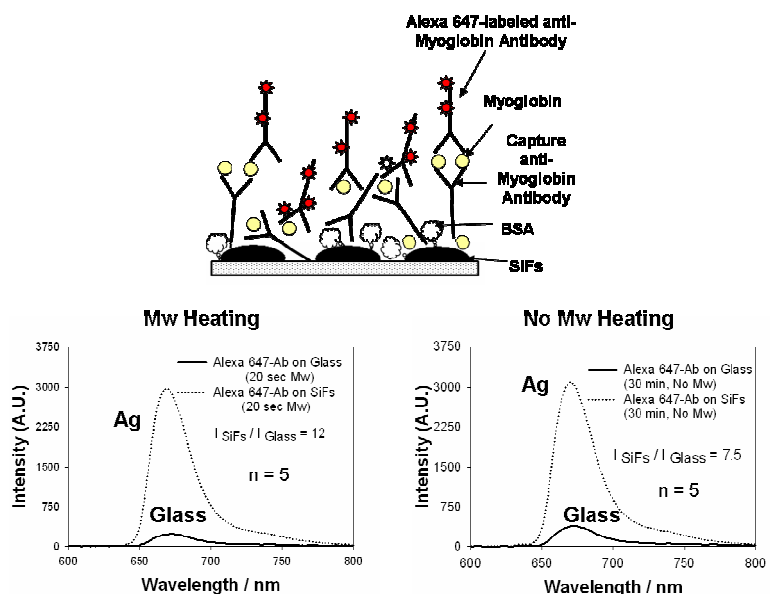
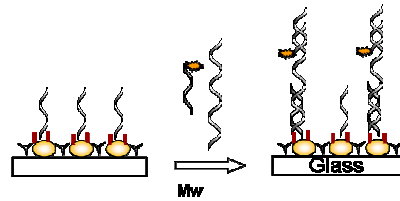


Fig. 5. Top Microwave-Accelerated Metal-Enhanced Fluorescence (MAMEF) Myoglobin immunoassay. Fluorescence intensities of the myoglobin immunoassay in the presence and absence of silver after low power microwave heating (Bottom-Left) and with no microwave heating (Bottom-Right). These results were obtained on a silvered glass microscope slides rather than HTS wells where one would get the same results. Adapted from reference 15.

3.5 MAMEF-based Anthrax Detection (DNA Detection)

The MA-MEF based ultra fast detection of Anthrax was demonstrated by using a synthetic Anthrax DNA in the nanomolar concentration range. First the silver-deposited glass surfaces were converted into MA-MEF assay platforms for the ultra fast detection of target Anthrax DNA. This was achieved by attaching an anchor probe that only recognizes the target Anthrax DNA after the preparation of SiFs on glass surfaces (Figure 6-Top). The basic attachment chemistry is similar to that used for surface plasmon resonance gold chips (24) and is based on the interaction of silver and sulfhydryl group on the anchor probe. In order to increase the efficiency of binding of the anchor to the target Anthrax DNA, at the sulfhydryl end, a 6 nucleotide region with inherent flexibility, which does not bind to the target Anthrax DNA made of Thymidines (25), was added. Moreover, to increase the sensitivity of the assay by reducing the undesired binding of Anthrax DNA to the assay platform, additional surface modification procedures were employed. These procedures involved the treatment of the unsilvered glass and silver surface that the anchor probe is not present by chemicals that resist the undesired binding of Anthrax DNA.



● : Silver Island Films (SiFs) γ : Succinic Anhydride : TAMRA-labeled 22-mer Oligo
| : 2-Amino(ethoxy)ethanol : Thiolated 21-mer Oligo : Target 49-mer Oligo

Concentration-dependent fluorescence emission data (Figure 6-Bottom-Left) obtained only after 30 seconds of microwave heating show an intensity increase as increasing concentration of Anthrax DNA is hybridized on the surface assay platform. Control experiments, where the surface-bound anchor probe is omitted, shows minimal emission intensity (less than that of the normal assay) despite the concentration of the Anthrax DNA being

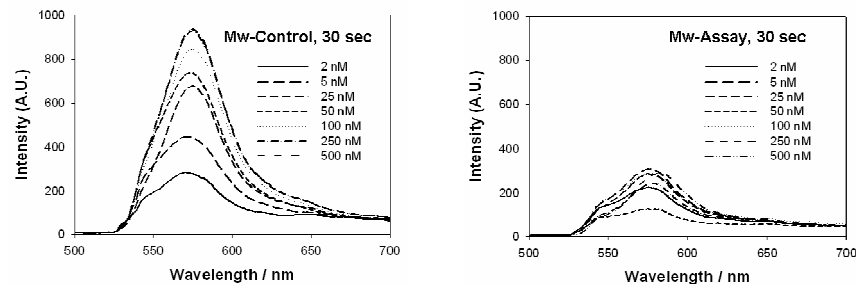


Fig. 6. Top-Microwave Accelerated Metal-Enhanced Fluorescence-based sensing scheme for fast and sensitive DNA target detection. Bottom-Left-Emission spectra of TAMRA-Oligo as a function of target Anthrax concentration after 30 s low power microwave heating; Mw-Microwave heating.

increased (Figure 6- Bottom-Right). A plot of the intensity at the peak of orange emission (at 585 nm) for the data obtained in the assay and the control experiment (data not shown) shows that the emission intensity at 585 nm is directly related to the solution Anthrax DNA concentration for values from 2 to 500 nM.

There are several key features of the data obtained for synthetic Anthrax DNA. First, the applicability of MA-MEF technology to a three-piece DNA detection system (one capture, one detector and the target DNA) without any modifications to the target DNA sample was demonstrated. Second, through control experiments the design of the assay platform was proven to be effective in minimizing the non-specific binding of Anthrax DNA to the surface other than the anchor probe. Third, these data show that Anthrax DNA can be detected with a signal-to-noise ratio > 3 for concentrations down to 5 nM.

3.6 Microwave-Accelerated Surface Plasmon-Coupled Directional Luminescence: Application to Fast and Sensitive Assays in Buffer, Human Serum and Whole Blood

So far, MAMEF technology has been described for assays constructed on non-continuous silver nanoparticles. It was previously shown that a new technology, Surface Plasmon Fluorescence Spectroscopy (SPFS) (26), which utilizes continuous metal films, provides researchers with better assay sensitivity. In this regard, we have shown the applicability of microwave heating to SPFS and subsequently named the amalgamation of these techniques as Microwave-Accelerated Surface Plasmon Coupled Luminescence (MA-SPCL). The proof-of-principle of MA-SPCL technique was demonstrated for fast and sensitive bioassays in buffer, serum and whole blood using quantum dots as luminescence

reporters. In this regard, a model bioassay based on the well-known interactions of biotin and streptavidin is used. Using MA-SPCL, the bioassay was kinetically completed within 1 minute with the use of low power microwave heating as compared to the identical bioassay which took in excess of 30 minutes to reach >95% completion at room temperature, a 30-fold increase in assay kinetics. The luminescence emission from the quantum dots was coupled to surface plasmons of the gold film, enabling the detection of the luminescence emission in a highly directional fashion as compared to the normal isotropic emission, for enhanced sensitivity and detection.

In order for the gold-coated glass slides to be used in MA-SPCL bioassays, they have to withstand the microwave heating while the bioassay is being driven to completion, as well as further physical treatments, such as multiple buffer washing steps. Thus, at first, the feasibility of the gold coated glass slides, like those commonly used in SPSF (26) and Surface Plasmon Resonance (24) were tested for their use in MA-SPCL assays via exposure to microwaves. Figure 7-left shows the photograph of typically used gold-coated glass slide

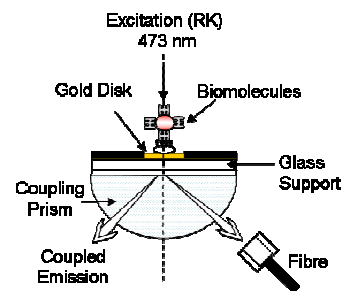
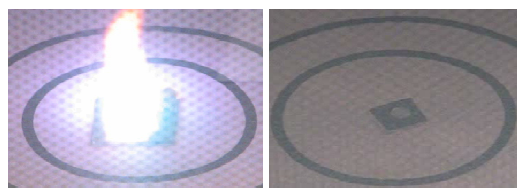


Fig. 7. Photographs of gold-coated glass slides during microwave heating. (Left) - the glass slide with a continuous gold coating, and (Middle) - the glass slide with a 5 mm diameter gold disk. While the glass slide with a continuous gold coating sparks, the glass slide featuring a gold disk is not affected during microwave heating. Right Optical set-up for Microwave-Accelerated Surface Plasmon Coupled Luminescence (MA-SPCL) bioassays. The sample is excited directly in the reverse Kretschmann (RK) configuration. The assay is undertaken on the gold-coated glass slide, which is attached to the glass prism with index matching fluid. The two arrows on the left side show the directional coupled luminescence emission. Figure is not drawn to scale.

during microwave heating. When exposed to microwaves, the glass slide with a continuous gold coating sparks and is destroyed within seconds, proving them not to be useful with MA-SPCL bioassays. However, the glass slide featuring only a 5 mm gold disk and a black body, made from the same gold-coated glass slide used in Figure 7-Left, is not destroyed even after continuous (1 minute) and repetitive (5 times) microwave heating, Figure 7-Middle. This was possible due to 1) the fact that the surface area of the gold disks is smaller than the area required for the surface charge buildup and eventual destruction of the gold coating, and 2) the black body used absorbs an excess of the microwaves, providing additional protection for the gold coating. In light of these observations, only the glass slide featuring a 5 mm gold disk can be used for MA-SPCL bioassays, a significant observation and finding, and attributed to the size of the disk being sub-wavelength with respect to the microwaves.

To demonstrate MA-SPCL bioassays on small disk gold films, we employed a model assay (Figure 7-Right) based on the well-known interactions of biotin and avidin. The model protein assay was constructed with biotinylated-BSA surface modified gold films and streptavidin-modified quantum dots, and run both at room temperature and microwave accelerated (heated). The angular distribution of luminescence for 33 nM of quantum dots used in the MA-SPCL assay, both microwave heated (Mw, 1 minute) and run at room temperature (RT, 30 minutes) was obtained (data not shown).

In order to demonstrate the utility of MA-SPCL assay in a quantitative manner, the MA-SPCL assay was undertaken with varying concentrations of quantum dots-streptavidin, 10-1250 nM. Figure 8-Top-Left shows the emission spectra of varying concentrations for the quantum dots used in the MA-SPCL assay measured at 217 degrees, as well as the real-color photograph obtained through the same emission filter used in the experiments. The calibration curve (intensity at 665 nm vs. concentration of the quantum dots) is obtained from the Figure 8-Top-Left, and is shown in Figure 8-Top-Right. As can be seen from Figure 8, the intensity measured at 655 nm and 217 degrees in the MA-SPCL setup increases with the increasing concentration of quantum dots-streptavidin (Figure 8-Top), and followed a linear trend within the range of quantum dots-streptavidin concentration used (Figure 8-Top). A real-color photograph taken through an emission filter at 217 degrees is also given as a visual evidence for the surface plasmon coupled luminescence. To further demonstrate the benefits of the MA-SPCL technique for whole blood assays, the assay using quantum dots-streptavidin was repeated in whole blood both with microwave heating and at room temperature for comparison. Figure

8-Bottom shows the MA-SPCL assay (Mw, 1 minute) and the SPCL assay at room temperature (RT, 20 min) performed in whole blood measured at 217 degrees.

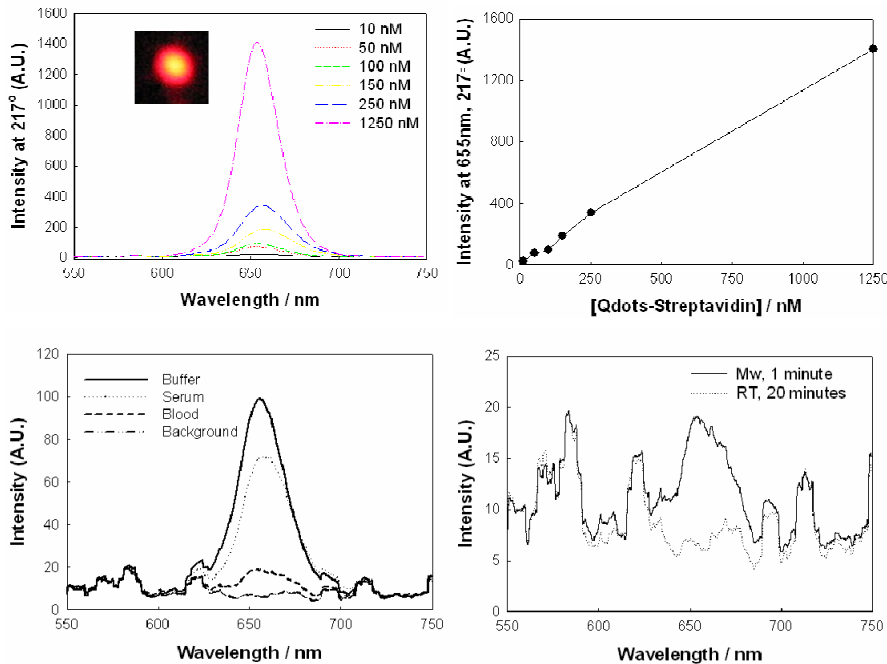


Fig. 8. Top-Left- The emission spectra of varying concentrations of quantum dots used in the MA-SPCL assay measured at 217 degrees. Top-Right-The calibration curve, intensity at 665 nm vs. concentration of the quantum dots, is obtained from the top figure. Bottom-Left- The emission spectra of 33 nM quantum dots used in the MA-SPCL assay measured at 217 degrees in different media. Bottom-Right- The MA-SPCL assay (Mw, 30 seconds) and at room temperature (RT, 20 min) performed in whole blood measured at 217 degrees.

While the assay that was microwave heated (accelerated) for 1 minute yielded a measurable signal, the assay that was undertaken at room temperature for 20 minutes did not yield any signal. This is due to the fact that the whole blood used in the assay at room temperature coagulated within 10 to 15 minutes, entrapping the quantum dots, resulting in no luminescence signal change. On the other hand, when the whole blood is microwave heated for 1 minute, significantly less coagulation of the blood occurred enabling the assay to be completed, a significant benefit to our approach to whole blood assays. It is important to note that the concentration of the quantum dots (33 nM) used in the whole blood MA-SPCL assay, was closer to the lower detection limit found here (Figure 8-Top), promising the use of the MA-SPCL assay in whole blood for a concentration range similar to that of the assay

in buffer. This is made possible by the use of microwave heating that significantly reduces the assay time, so that the assay could be completed in whole blood before the blood coagulates, while also decreasing the non-specific interactions. In this regard, numerous reports have employed microwaves and whole blood (27), strongly suggesting that whole blood components are not damaged by microwave exposure.

3.7 Microwave-Accelerated Ultra-Fast Nanoparticle Aggregation Assays using Gold Colloids

In a separate study, we have also demonstrated the proof-of-principle of the Microwave-Accelerated Aggregation Assay (MA-AA) technology, which shortens a solution based nanoparticle aggregation assays' run time to within seconds (> 100-fold increase in kinetics) with microwave heating. In this regard, we have used a model aggregation assay based on the well-known interactions of biotin and avidin (Figure 9-Top). Biotinylated gold colloids were aggregated in solution with the addition of streptavidin, which takes 20 minutes at room temperature to reach > %90 completion and only 10 seconds with microwave heating. The initial velocity (after 1 sec microwave heating) of the biotinylated gold colloids reaches up to 10.5 m/s, which gives rise to greater sampling of the total volume, but not an increase in bulk temperature. The room temperature steady-state velocity of the colloids was < 0.5 $\mu\text{m/s}$. In control experiments, where streptavidin pre-incubated with *D*-biotin in solution is added to biotinylated gold colloids and microwave heated, gold colloids did not aggregate demonstrating that non-specific interactions between biotinylated gold colloids and streptavidin was negligible.

As shown by Kogan *et al.* (28) when exposed to weak microwave fields, gold colloids absorb and dissipate the electromagnetic energy at higher frequencies (> 8 GHz) without any bulk heating due to the minimal absorption by water. In this regard, to determine the effect of microwave heating (2.45 GHz) on the surface plasmon resonance of gold colloids, absorption spectrum of gold colloids with varying concentrations was measured (data not shown).

We found out that when exposed to 10 seconds microwave heating the absorption spectrum of gold colloids remains unchanged for all the concentrations used here. This finding indicates that any change in absorption spectrum of the colloids in the microwave-accelerated aggregation assays is due the other factors (i.e., binding events, etc). The effect of temperature on gold colloids was also studied by employing a conventional heating method. Similarly, the absorption spectrum of gold colloids remains unchanged after conventional heating (data not shown).

Figure 9 shows the change in absorbance of biotinylated-BSA 20 nm gold colloids (cross linked by different additions of streptavidin, both without (20 min incubation) and after low power microwave heating), as well as the change in absorbance at 650 nm for both the room temperature incubated (1 and 20 min) and microwave heated (10 sec) samples. The extent of the aggregation of biotinylated gold colloids was almost identical both at room temperature (20 min) and with microwave heating, while the extent of aggregation of biotinylated gold colloids was significantly less than either of these cases at room temperature when run for 1 minute (Figure 9-D). These results indicate that low power microwave heating of the gold colloids results in the completion of the aggregation process in \approx 10 seconds, a 120-fold increase in kinetics compared to the room temperature assay.

A recent report on the effects of microwaves (800 W, at 2.45 GHz for 10 sec) on proteins, showed that microwave photons interact with tertiary structure of proteins but the chemical bonds are unaffected (29). In addition, it was reported that microwaves (100 mW, 12 GHz for 8 hours) accelerated the macromolecular aggregation of amyloid beta protein as well as dissolution of the protein aggregates in the presence of gold colloids with 99.99% of the microwave energy being absorbed by the gold colloids since water does not absorb the electromagnetic energy at these wavelengths, i.e., at 12 GHz. (28) In another report by us (11), Fluorescence Resonance Energy Transfer studies on proteins in close proximity to silver nanoparticles revealed that proteins do not denature when exposed to microwaves (140 W, at 2.45 GHz for 30 sec) despite the absorption of electromagnetic energy by water at 2.45 GHz that resulted in an increase in the temperature of the bulk medium by 8°C. This was possible by the attenuation of the microwaves with the microwave absorbing material present around the sample chamber (11).

Here, the microwave power used for the aggregation assay was 140 W (at 2.45 GHz for 10 sec), which resulted in an increase in the temperature of the bulk medium by 5°C (data not shown) primarily due to the direct absorption of energy by water at 2.45 GHz. The heat absorption and loss by the 0.8 nM gold colloids was calculated to be 10560 J / ml. The dissipated heat from the gold colloids is much larger than the energy required for formation of biotin-avidin complex. While we can not be certain about the extent of dissipated energy from the colloids that results in increase in kinetic energy of gold colloids and increase in bulk temperature (due to dissipation of the absorbed energy by the gold colloids as heat to the solution), at this time, we hypothesize that a significant part of the dissipated energy from the gold colloids is contributing to kinetic energy, which results in the ability of the biotinylated gold colloids to move about the solution

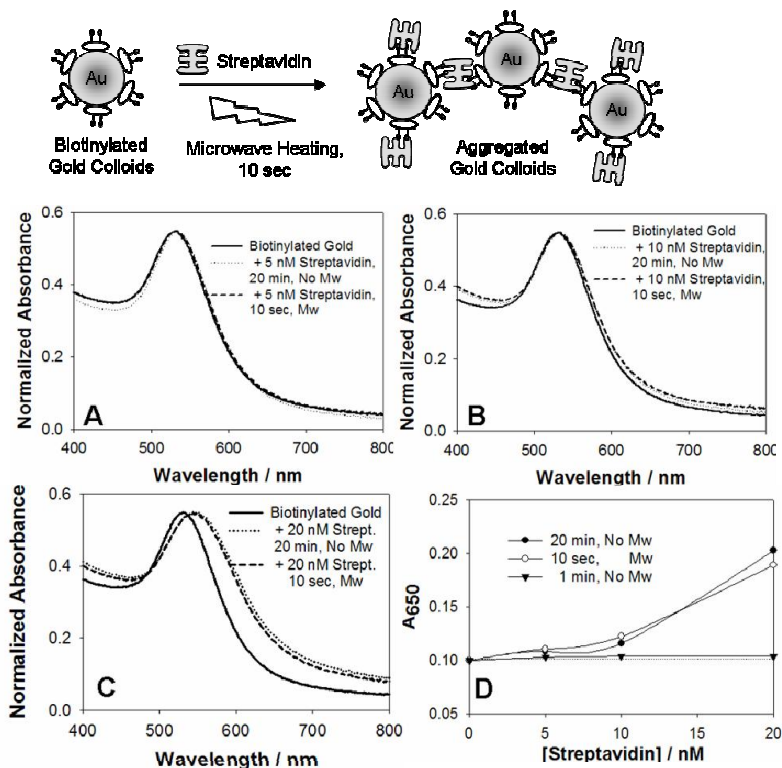


Fig. 9. Top- Model MA-AA using gold colloids. Biotinylated-BSA coated 20 nm gold colloids cross linked by streptavidin. Change in absorbance of biotinylated-BSA 20 nm gold colloids crosslinked by different additions of streptavidin, both without (20 min incubation) and after low power microwave heating. A – 5 nM, B – 10 nM and C – 20 nM streptavidin additions. Plot D shows the change in absorbance at 650 nm for both the room temperature incubated and microwave heated samples.

volume at increased velocities. However, we note that as previously hypothesized by Hamad-Schifferli *et al.* (30), the increase in kinetic energy of gold colloids is a result of induced dipole torque on the colloids. The initial velocity (after 1 sec microwave heating) of the biotinylated gold colloids reaches up to 10.5 m/s, which gives rise to greater sampling of the total volume but not an increase in bulk temperature. In this regard, as the biotinylated gold colloids collide with free streptavidin molecules (and other biotinylated gold colloids) some of the energy is lost due to collisions and some for the formation of the biotin-streptavidin complex. As the biotinylated gold colloids-streptavidin aggregates increase in size, more energy is used, and ultimately, the aggregation process stops after all dissipated energy is used.

In order to prove our hypothesis that the energy absorbed by gold colloids is dissipated local to the colloids, and this energy dissipation does not cause bulk heating, the temperature distribution around the gold colloids was calculated and plotted in Figure 10-Left, and it was found to be in the order of a few microKelvin. Figure 10 also shows the spatial distribution of the temperature rise inside and outside the gold colloids which indicates the efficient dissipation of heat by the gold colloids without causing bulk heating. Thus, the primary source of increase in bulk temperature is due to the absorption of energy at 2.45 GHz directly by water. Thus, the only source of increase in bulk water temperature is the absorption of energy at 2.45 GHz, which we believe probably accounts, to some extent, for the faster aggregation kinetics. As shown before (28), such a rapid acceleration in temperature did not denature the streptavidin molecules and thus the microwave-accelerated aggregation assays using gold colloids was made possible.

As a useful tool for other nanoparticle workers, and to show broad applicability of our approach one can also calculate the expected temperature rise at the surface of the colloids ($r = R$) for various gold colloids sizes and various electromagnetic energy frequencies, Figure 10-Middle. As shown in Figure 10-Middle, the temperature rise increase with the increase in the size of the gold colloids and the electromagnetic energy frequency. This shows that different size of gold colloids as well different microwave sources can be used in MA-AA assays without causing an increase in the bulk temperature. One can also calculate the initial velocity of the gold colloids right after ($t=1$ second) the absorption of electromagnetic energy (after 1 second, from kinetic energy, $KE = PT$, 1 sec). As shown in Figure 10-Right, the initial velocity of the gold colloids increases with the increase in the size of the gold colloids and the electromagnetic energy frequency. Different size of gold colloids (along with different electromagnetic energy) could be used in MA-AA assay for even faster kinetics.

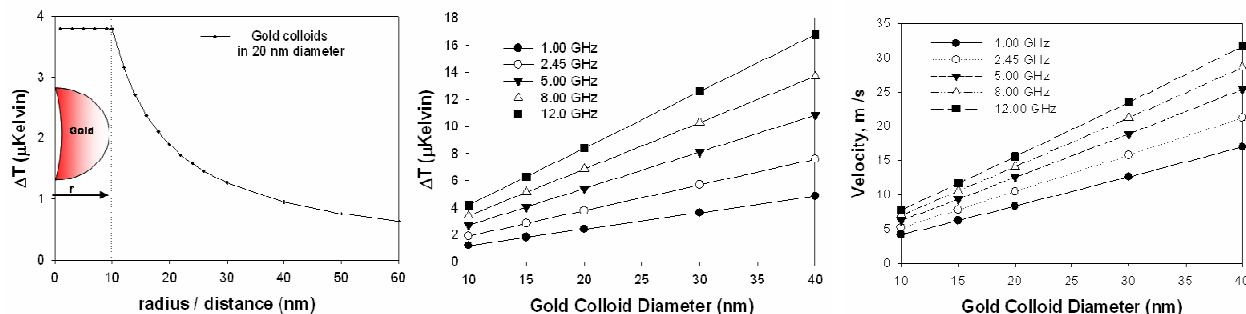


Fig. 10. Left- Spatial distribution of temperature rise (ΔT) inside ($r =$ to 10 nm) and outside ($r = 10$ to 60 nm) the surface of gold colloids at equilibrium. Note that while the temperature rise inside the gold colloids is constant, the temperature rise diminishes as the distance from the surface of gold colloids increases. Middle- Calculated rise in temperature (ΔT) close to the surface ($r=R$) of various size of gold colloids using various frequencies of electromagnetic energy. Right- Calculated initial velocity of the biotinylated gold colloids after 1 sec of microwave heating at different frequencies.

4. CONCLUSIONS

In conclusion, we have summarized our current work on microwave-accelerated plasmonics. This summary included results from seven different papers. More specifically, we have demonstrated utilization of MAMEF technology using a model assay sensing platform for potential use in HTS 96-well plate formats. This new approach provides for both ultra fast and brighter assays as well as immunoassays in HTS platforms, which is likely to find popular use. The new MAMEF approach combines the use of silver nanostructures to optically amplify fluorescence signatures, a new near-field phenomenon, with the use of low power microwaves to kinetically accelerate the assays. The microwaves do not perturb the silver nanostructures, but simply increase the mass transport of protein to the plate well-bottoms. We also

found that the microwaves do not perturb the assay proteins, but simply increase the mass transport of protein to the silvered surface. For the model assay described here, the use of Microwave-Accelerated Metal-Enhanced Fluorescence (MAMEF) provides for a 10-fold brighter and a 90-fold quicker assay.

We have demonstrated the application of the MAMEF technology to a model myoglobin immunoassay for the potential rapid and sensitive detection of a myocardial infarction, where myoglobin is one of four cardiac markers typically used for the assessment of myocardial infarction (31). The assay demonstrated can readily detect 100 ng/ml of myoglobin in 20 seconds, from only 50 μ L of fluid. The S/N of the assay is about 100-times above the background for 100 ng/ml myoglobin, which suggests that this approach could equally be used to detect other more specific cardiac markers, such as either Troponin I or T, which have clinical cut off levels of only a few ng/ml (31).

The feasibility of the MA-SPCL technique was demonstrated with a model assay using streptavidin conjugated quantum dots and surface-bound biotinylated BSA. With the MA-SCPL technique, 10-1250 nM of streptavidin was detected within 1 minute, which corresponds to \approx 30-fold faster kinetics as compared to the assay undertaken at room temperature. The accelerated assay kinetics was made possible by the heating of a gold disk by microwaves, resulting in a slight increase in the bulk solution temperature, with higher temperature jumps close-to the gold surface. Moreover, highly directional coupled luminescence emission from quantum dots enabled the realization of sensitive luminescence measurements. The combined effect of microwaves for faster assay kinetics with surface plasmon-coupled luminescence for sensitive measurements also made possible the demonstration of the use of MA-SPCL technique for assays to be run in complex media such as human serum and whole blood, while the same assay *could not be performed* at room temperature due to the coagulation of blood. In the MA-SPCL assay run in serum and whole blood, the luminescence intensity from 33 nM quantum dots was 75% and 20% that of the luminescence intensity from the assay run in buffer, with a signal to noise ratio of 12.5 and 3, respectively.

Finally, we have demonstrated the Microwave-Accelerated Aggregation Assay technique, using a standard household microwave generator and gold colloids as localized energy "sink", for ultra fast solution based aggregation assays. We have found that the assay's run time is reduced from minutes to within a few seconds, a result of increased velocity (from in the order of μ m/s to 10 m/s) of the gold colloids. Our experimental observations and calculations show that the bulk heating of the water is negligible by the nanoparticles, the water directly heated by microwaves at 2.45 GHz. In addition, our calculations show that 5°C increase in bulk solution temperature, does not solely account for the fast reaction times, where the significant increase in nanoparticle velocity is thought to account for this. With an initial assay velocity of > 10.5 m/s directly after heating, the particles are thought to sample a greater volume per unit time, accounting for the increased assay kinetics. We have also provided additional charts showing both the temperature increase and velocity, for a range of microwave frequencies and nanoparticle size.

5. ACKNOWLEDGMENT

This work was supported by the Middle Atlantic Regional Center of Excellence for Biodefense and Emerging Infectious Diseases Research (NIH NIAID - U54 AI057168). The authors would like acknowledge UMBI and IoF for salary support. Additional salary support to CDG from National Center for Research Resources, RR008119 is also acknowledged.

REFERENCES

1. K. Aslan, R. Badugu, J. R. Lakowicz and C. D. Geddes, "Metal-enhanced fluorescence from plastic substrates," *Journal of fluorescence* 15(2), 99-104 (2005)
2. K. Aslan, I. Gryczynski, J. Malicka, E. Matveeva, J. R. Lakowicz and C. D. Geddes, "Metal-enhanced fluorescence: an emerging tool in biotechnology," *Current Opinion in Biotechnology* 16(1), 55-62 (2005)
3. K. Aslan, P. Holley and C. D. Geddes, "Metal-enhanced fluorescence from silver nanoparticle-deposited polycarbonate substrates," *Journal of Materials Chemistry* 16(27), 2846-2852 (2006)
4. K. Aslan, J. R. Lakowicz and C. D. Geddes, "Rapid deposition of triangular silver nanoplates on planar surfaces: Application to metal-enhanced fluorescence," *Journal of Physical Chemistry B* 109(13), 6247-6251 (2005)
5. K. Aslan, J. R. Lakowicz, H. Szmajnski and C. D. Geddes, "Enhanced ratiometric pH sensing using SNAFL-2 on silver island films: Metal-enhanced fluorescence sensing," *Journal of fluorescence* 15(1), 37-40 (2005)
6. K. Aslan, Z. Leonenko, J. R. Lakowicz and C. D. Geddes, "Fast and slow deposition of silver nanorods on planar surfaces: Application to metal-enhanced fluorescence," *Journal of Physical Chemistry B* 109(8), 3157-3162 (2005)

7. J. Malicka, I. Gryczynski, Z. Gryczynski and J. R. Lakowicz, "DNA hybridization using surface plasmon-coupled emission," *Analytical chemistry* 75(23), 6629-6633 (2003)
8. J. Malicka, I. Gryczynski and J. R. Lakowicz, "DNA hybridization assays using metal-enhanced fluorescence," *Biochemical and biophysical research communications* 306(1), 213-218 (2003)
9. Y. X. Zhang, K. Aslan, S. N. Malyn and C. D. Geddes, "Metal-enhanced phosphorescence (MEP)," *Chemical Physics Letters* 427(4-6), 432-437 (2006)
10. M. H. Chowdhury, K. Aslan, S. N. Malyn, J. R. Lakowicz and C. D. Geddes, "Metal-enhanced chemiluminescence," *Journal of fluorescence* 16(3), 295-299 (2006)
11. K. Aslan and C. D. Geddes, "Microwave-accelerated metal-enhanced fluorescence: Platform technology for ultrafast and ultrabright assays," *Analytical chemistry* 77(24), 8057-8067 (2005)
12. K. Aslan, Z. Leonenko, J. R. Lakowicz and C. D. Geddes, "Annealed silver-island films for applications in metal-enhanced fluorescence: Interpretation in terms of radiating plasmons," *Journal of fluorescence* 15(5), 643-654 (2005)
13. L. A. Hemmila, *Applications of Fluorescence in Immunoassays*, John Wiley and Sons, New York (1992).
14. K. Aslan, S. N. Malyn and C. D. Geddes, "Fast and sensitive DNA hybridization assays using microwave-accelerated metal-enhanced fluorescence," *Biochemical and biophysical research communications* 348(2), 612-617 (2006)
15. K. Aslan and C. D. Geddes, "Microwave-accelerated Metal-enhanced Fluorescence (MAMEF): Application to ultra fast and sensitive clinical assays," *Journal of fluorescence* 16(1), 3-8 (2006)
16. K. Aslan, J. R. Lakowicz and C. D. Geddes, "Nanogold plasmon resonance-based glucose sensing. 2. Wavelength-ratiometric resonance light scattering," *Analytical chemistry* 77(7), 2007-2014 (2005)
17. S. Link and M. A. El-Sayed, "Spectral properties and relaxation dynamics of surface plasmon electronic oscillations in gold and silver nanodots and nanorods," *Journal of Physical Chemistry B* 103(40), 8410-8426 (1999)
18. A. G. Whittaker and D. M. P. Mingos, "Microwave-Assisted Solid-State Reactions Involving Metal Powders and Gases," *Journal of the Chemical Society-Dalton Transactions* 16), 2541-2543 (1993)
19. K. Aslan, P. Holley and C. D. Geddes, "Microwave-Accelerated Metal-Enhanced Fluorescence (MAMEF) with silver colloids in 96-well plates: Application to ultra fast and sensitive immunoassays, High Throughput Screening and drug discovery," *Journal of Immunological Methods* 312(1-2), 137-147 (2006)
20. M. Wilchek and E. A. Bayer, "Applications of avidin-biotin technology: literature survey," *Methods Enzymol* 184(14-45) (1990)
21. C. D. Geddes, K. Aslan, I. Gryczynski, J. Malicka and J. R. Lakowicz, "Noble-Metal Surfaces for Metal-Enhanced Fluorescence," in *Reviews in Fluorescence 2004* C. D. Geddes and J. R. Lakowicz, Eds., pp. 365-401, Kluwer Academic/Plenum Publishers, New York (2004).
22. D. Adam, "Microwave chemistry: Out of the kitchen," *Nature* 421(6923), 571-572 (2003)
23. J. R. Lakowicz, *Principles of Fluorescence Spectroscopy*, Kluwer Academic, New York (1999).
24. B. Liedberg, I. Lundstrom and E. Stenberg, "Principles of Biosensing with an Extended Coupling Matrix and Surface-Plasmon Resonance," *Sensors and Actuators B-Chemical* 11(1-3), 63-72 (1993)
25. S. D. Goodman and O. Kay, "Replacement of integration host factor protein-induced DNA bending by flexible regions of DNA," *Journal of Biological Chemistry* 274(52), 37004-37011 (1999)
26. T. Liebermann and W. Knoll, "Surface-plasmon field-enhanced fluorescence spectroscopy," *Colloids and Surfaces A-Physicochemical and Engineering Aspects* 171(1-3), 115-130 (2000)
27. J. Hirsch, A. Menzebach, I. D. Welters, G. V. Dietrich, N. Katz and G. Hempelmann, "Indicators of erythrocyte damage after microwave warming of packed red blood cells," *Clinical chemistry* 49(5), 792-799 (2003)
28. M. J. Kogan, N. G. Bastus, R. Amigo, D. Grillo-Bosch, E. Araya, A. Turiel, A. Labarta, E. Giralt and V. F. Puntes, "Nanoparticle-mediated local and remote manipulation of protein aggregation," *Nano Letters* 6(1), 110-115 (2006)
29. H. Bohr and J. Bohr, "Microwave-enhanced folding and denaturation of globular proteins," *Physical review* 61(4 Pt B), 4310-4314 (2000)
30. K. Hamad-Schifferli, J. J. Schwartz, A. T. Santos, S. G. Zhang and J. M. Jacobson, "Remote electronic control of DNA hybridization through inductive coupling to an attached metal nanocrystal antenna," *Nature* 415(6868), 152-155 (2002)
31. K. Aslan and C. D. Geddes, "Microwave Accelerated and Metal Enhanced Fluorescence Myoglobin Detection on Silvered Surfaces: Potential Application to Myocardial Infarction Diagnosis," *Plasmonics* 1(1), 53-59 (2006)